Proteomics
Proteomics and Systems Biology
www.proteomics-journal.com

Absolute Quantification of Proteins in the Eye of *Drosophila melanogaster*

*Bharath Kumar Raghuraman, Sarita Hebbar, Mukesh Kumar, HongKee Moon, Ian Henry, Elisabeth Knust, and Andrej Shevchenko**

Absolute (molar) quantification of proteins determines their molar ratios in complexes, networks, and metabolic pathways. MS Western workflow is employed to determine molar abundances of proteins potentially critical for morphogenesis and phototransduction (PT) in eyes of *Drosophila melanogaster* using a single chimeric 264 kDa protein standard that covers, in total, 197 peptides from 43 proteins. The majority of proteins are independently quantified with two to four proteotypic peptides with the coefficient of variation of less than 15%, better than 1000-fold dynamic range and sub-femtomole sensitivity. Here, the molar abundance of proteins of the PT machinery and of the rhabdomere, the photosensitive organelle, is determined in eyes of wild-type flies as well as in *crumbs* (*crb*) mutant eyes, which exhibit perturbed rhabdomere morphogenesis.

1. Introduction

Proteomics is quantitative. A plethora of analytical methods have been developed to determine fold changes in the abundance of thousands of proteins in series of biological or clinical experiments (reviewed in refs. [1–3]). Relative quantification is a common approach for surveying global changes in the proteome and pinpointing the most affected proteins. However, it does not determine their absolute (molar) abundances and therefore the levels of different proteins cannot be compared directly.

Absolute (molar) quantification (reviewed in refs. [4–7]) typically relies on exactly known quantities of isotopically labelled peptide standards that are identical to the corresponding peptides from endogenous proteins. Knowing molar concentration of individual proteins in biofluids (e.g., blood plasma) is critical for diagnostics and monitoring the diseases. Also, molar concentrations elucidate stoichiometry of multi-protein assemblies, or molar ratios between proteins within metabolic and signaling networks and provide insight in their molecular composition and regulation. Last but not least, absolute quantification relates the abundances of proteins to other biomolecules such as lipids or DNA and facilitates systems biology modeling of chemical processes underlying development and metabolism.[8]

MS Western workflow quantifies gel-separated proteins by in-gel co-digestion with an isotopically labeled QconCAT-like protein chimera followed by LC-MS/MS.[9] MS Western requires no purification of the chimera and relates the molar abundance of all proteotypic peptides (i.e., unique peptides per each protein that are consistently detected by LC-MS/MS) to a single reference protein (typically, BSA). The use of 1D SDS PAGE circumvents limited solubility and purity of large (>250 kDa) chimeric proteins (CPs). Since proteins could be solubilized and recovered in the presence of SDS the method prompts for unbiased quantification of membrane proteins without compromising the low femtomole to attomole sensitivity. We reasoned that the capacity of MS Western to accurately quantify dozens of soluble and membrane proteins in parallel could also be instrumental to better understand the organization of tissues or entire organs and how the proteome bridges their morphology with physiological function.

The fly eye is a valuable model to unravel the basis of photoreceptor functions and visual impairment, since many genes and proteins involved in phototransduction, eye morphology, and homeostasis are highly conserved.[10,11] The fly eye is a stereotypically organized organ, consisting of 750–800 repeated hexagonal units, called ommatidia. Each ommatidium consists of 20 epithelial cells including 8 photoreceptor cells (PRC) (schematized in **Figure 1**A) and 12 accessory cells. The plasma membrane of the highly polarized PRCs is sub-divided, on the basis of its morphology and function, into the basal domain, junctional domain, sub-apical, and apical domains (Figure 1A,B). The most

B. K. Raghuraman, Dr. S. Hebbar, Dr. M. Kumar[+], Dr. H. Moon, Dr. I. Henry, Prof. E. Knust, Dr. A. Shevchenko
Max Planck Institute of Molecular Cell Biology and Genetics
Pfotenhauerstr. 108, Dresden 01307, Germany
E-mail: shevchenko@mpi-cbg.de
Dr. H. Moon, Dr. I. Henry
Centre for Systems Biology Dresden
Pfotenhauerstr. 108 Dresden 01307, Germany

The ORCID identification number(s) for the author(s) of this article can be found under https://doi.org/10.1002/pmic.201900049

[+]Present address: F.M. Kirby Neurobiology Center, Boston Children's Hospital and Department of Neurology, Harvard Medical School, Boston, MA

DOI: 10.1002/pmic.201900049

apical domain of a PRC, termed rhabdomere, is a F-actin-rich, microvilli-based membranous structure (Figure 1C) that is highly enriched with proteins of the phototransduction (PT) machinery.[12,13] The integrity and morphology of rhabdomeres critically depends, among other proteins, on the evolutionary conserved gene *crumbs* (*crb*). Perturbing Crb affects rhabdomere morphogenesis and, eventually, leads to retinal degeneration.[14–16] However, how the rhabdomere proteome is organized in general, and how Crb preserves rhabdomere integrity, is poorly understood. What is the quantitative composition of the PT protein machinery? How much of the light sensing protein rhodopsin along with other proteins of the transduction machinery could be "packed" into a healthy rhabdomere and does their amount change in improperly formed PRCs? How much Crb is required to make a stable rhabdomere that retains the rhodopsin mass? We answered these and other related questions by direct absolute quantification of proteins of the PT machinery and members of the Crb-complex in wild-type and genetically manipulated flies.

2. Results and Discussion

2.1. Rationale and Design of the Study

Our aim was to establish the quantitative relationship between proteins of the PT machinery and of the apical membrane-organizing Crumbs protein complex in different biological contexts. We first quantified the molar abundances of PT proteins in a normally developed and fully functional wild-type fly eye and computed their basal molar ratios. Next, we used a series of *crb* mutants exhibiting different severity of impairment in rhabdomere morphology and compared molar abundances and ratios of PT proteins with the wild type.

For the absolute quantification of proteins we employed the method of MS Western[9] that relies on GeLC-MS/MS and isotopically labelled QconCAT-like CP standards. For this study, we designed a 264 kDa CP that, in total, encompassed 43 unique proteins; 12 of those were known key players in PT (e.g., Opsin-Rh1 / NinaE and Gαq) and photoreceptor morphogenesis such as Crumbs (Crb), Chaoptin (Chp), Eyes Shut (Eys), and Prominin (Prom). Additionally, we included peptides from 31 proteins reflecting different aspects of fly physiology (e.g., cytoskeleton organization, oxidative stress, etc.). Each target protein was represented by two to four proteotypic peptides detected in preliminary GeLC-MS/MS analyses of total protein extract of dissected eyes; the CP also comprised six peptides from the reference protein BSA (Table S1 and Figure S1A,B, Supporting Information). An aliquot of *E. coli* lysate was subjected to 1D SDS PAGE, CP band excised, and used as a standard for protein quantification[9] (Figure S1C, Supporting Information) that was automated with MS Western Mass Filter software. The molar amounts of individual proteins were normalized per eye or per number of relevant cells expressing these proteins (Table S4, Supporting Information) according to published data. In line with previous estimates the size of eyes did not change in wild type flies and in *crumbs* mutants and was not considered during the normalization.[9] MS Western quantification covered more than 1000-fold difference in the molar abundance of target proteins starting at Titin (Sallismus; Sls) of 0.11 ±0.1 fmole/eye and up to Phosrestin-1 (Arr-2) of 364±12 fmole/eye (Figure 1D; Table S3, Supporting Information).

Significance Statement

MS Western elucidated the molar ratios of key proteins within phototransduction and rhabdomere organization networks.

2.2. Technical Merits of the Absolute Quantification of Eye Proteins

Precise protein quantities are key to derive their molar ratios in complexes and pathways. The 43 eye proteins quantified here differed by localization (cytoplasmic or membrane), molecular weight, hydrophobicity and expression level. The Pearson coefficient of correlation between technical replicates was 0.99 (Figure S2A, Supporting Information) and 0.8–0.98 between biological replicates for all mutants (Figure S2B, Supporting Information). Notable outliers in crb^{11A22} and crb^{8F105} were Actins, likely due to imprecise dissection of eyes from fly heads.

Absolute quantification methods often rely on several (commonly two) proteotypic peptides per each target protein. This, however, often leads to discordant estimates that could differ by more than twofold.[17,18] Therefore, it was customary to only use the highest of a few estimates implying that lower estimates are due to some undefined biased losses of corresponding peptide(s). While this might be acceptable for characterizing the expression levels of proteins, it does not lead to a reliable determination of molar ratios. In MS Western we used two to four peptides per each quantified protein and, in our experiments, the median CV for multiple peptide-based quantitation (MPQ) was below 10% (**Figure 2**), which is a significant improvement in quantification accuracy.

We also compared the relative abundance of unlabeled peptides and corresponding isotopically labelled peptides originating from endogenous proteins and from CP standard, respectively (**Figure 3**A–F). Relative abundances of peptides are independent of protein quantities and their concordance indicated that the 264 kDa chimera standard faithfully represented all target (including membrane) proteins and that the quantification was not biased by limited trypsin cleavage or an unexpected PTM. Even for proteins whose abundance was close to the methods LOQ (e.g., Titin/Sls), the relative abundances of "light" and "heavy" quantitypic peptides were concordant (Figure 3B).

2.3. The Molar Abundance of Actins, Opsin, and Crumbs in Fly Eyes

We first asked how abundant is the PT machinery in *Drosophila* eyes? We reasoned that the molar content (moles per eye) alone might not be informative unless compared to an intuitive and common cell marker. Rhodopsin (Rh1) and Actin are the two major components of the rhabdomere—the organelle housing the phototransduction machinery. Rh1 is the most abundant opsin

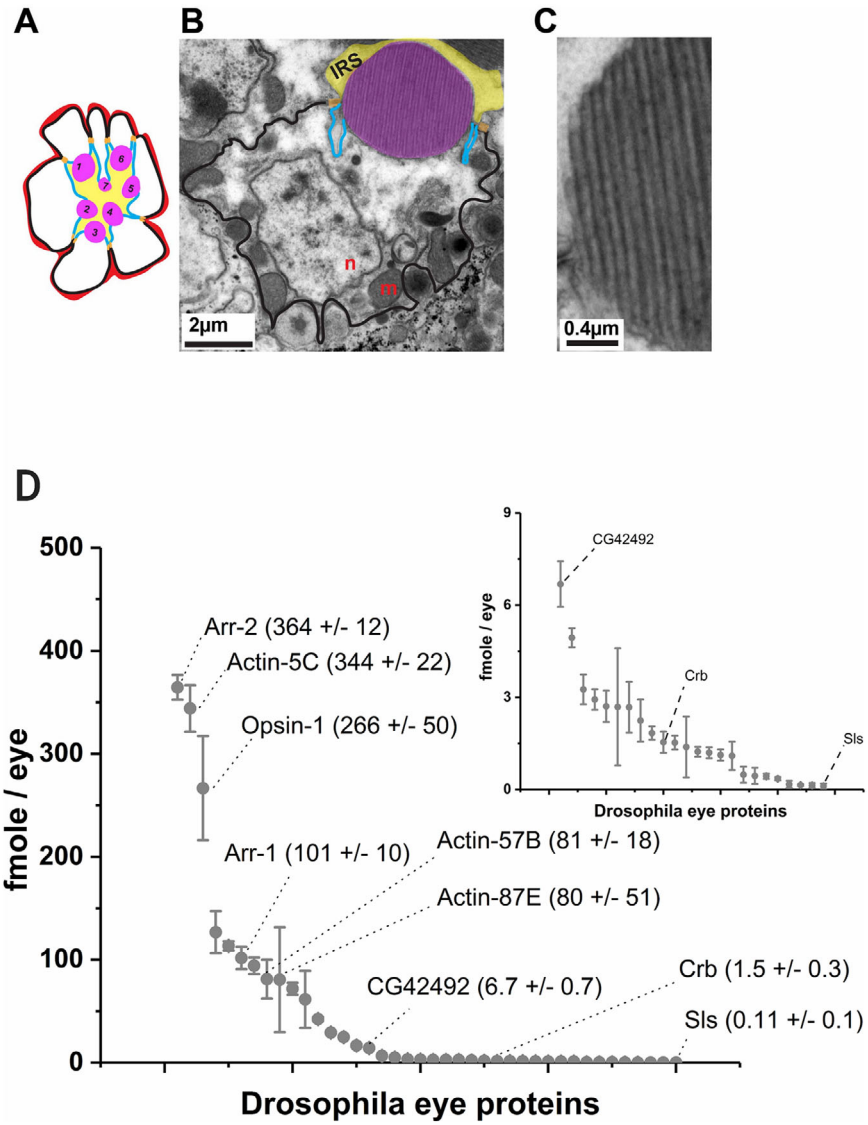

Figure 1. Absolute quantities of *Drosophila melanogaster* eye proteins. A) Cartoon depicting the cross-sectional view of a single ommatidium of the fly eye. Seven (1–7) photoreceptor cells (PRCs) and the surrounding pigment cells (in red) are shown here. The PRC plasma membrane is subdivided into distinct domains called basal (black), sub-apical (cyan) and the apical most (magenta, called rhabdomere). B) Electron microscopy image of a cross section of a PRC at the level of the nucleus (n) showing its distinct structural organization and its membrane domains. The apical most (pseudocolored in magenta) rhabdomere, the inter-rhabdomeral space (yellow), the sub-apical stalk (cyan), and the basal membrane (black) are indicated. The nucleus (n), mitochondria (m), and other organelles are more basally localized. C) Higher magnification electron microscopy image of a cross section of half a rhabdomere. The rhabdomere consists of closely apposed microvilli. D) Dynamic range and molar abundances (in fmole per eye) of the 43 quantified proteins in wild type (*Oregon R*) flies. Molar abundances of selected proteins (means +/− S.D. calculated for 2 biological replicates with two technical replicates) are shown in parenthesis next to protein names. Zoom view of the range of low abundant proteins is presented in the inset. Full list of molar abundances of all proteins is in Table S3, Supporting Information.

in the fly eye and comprises the Opsin protein (encoded by the gene *ninaE*[19]) conjugated to a chromophore. Decreased levels of Rh1 induced by mutating the *ninaE* gene,[20] or by removal of Vitamin A precursors[21] from the diet resulted in substantially smaller rhabdomeres (yet, this did not change the eye size) and suggested that levels of Rh1 and Actin are linked. We therefore referred the abundance of major PT protein Opsin first to actins, common components of the cytoskeleton, and second to Crumbs, a regulator of rhabdomere morphogenesis.

Opsin is amongst the three most abundant proteins we have quantified with an amount of 266 ± 51 fmoles/eye (Table S3, Supporting Information). Actin 5C at 344 ± 23 fmoles/eye is the most abundant among all actins, followed by Actin 87E (80±51 fmoles/eye) and Actin 57B (81± 19 fmoles/eye). Higher abundance of Actin 5C in comparison to Actin 87E and Actin 57B corroborates genetic evidence indicating that amongst the six *actin* genes in the *Drosophila* genome[22] *actin 5C* is critical for photoreceptor morphogenesis.

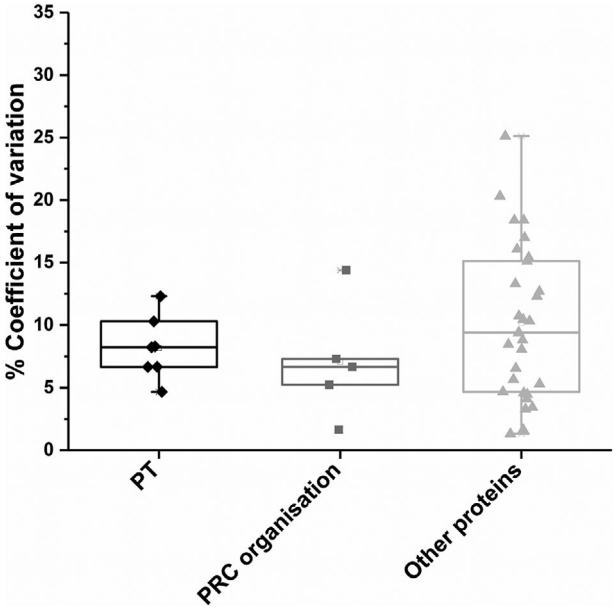

Figure 2. Concordant absolute quantification based on multiple peptides. Coefficient of variation of molar amounts of 43 proteins calculated using multiple proteotypic peptide per protein grouped into photo transduction proteins (PT), photo receptor cell (PRC) organizing proteins, and other proteins. Each data point represents one protein.

In case the expression pattern of a protein in the 16 000 cells[23] of the eye was known, we expressed its abundance in moles per cell (Table S4, Supporting Information). For instance, Opsin-1 is only expressed in six out of eight PRCs[19,24] and given the total number of ommatidia has been averaged to 800, this should be equivalent to 4800 cells in each eye and therefore the amount of Opsin is 56 amole/cell (Table S5, Supporting Information). Under the light conditions used here, the overwhelming majority of Opsin-1 is in the form of Rhodopsin-1 and resides in the rhabdomere. Assuming there are ≈40 000 microvilli per PRC (R1-R6),[25,26] this implies that there are approximately 836 Rh1 molecules per each microvillus. This corroborates with the rough estimate of 1000 Rh1 molecules per microvillus computed from particle density in ultrastructural images of rhabdomeres.[13]

Crumbs protein acts as a positional cue for rhabdomere[16,27] and its morphogenesis.[14,28] Furthermore, it is required for inhibiting light induced degeneration of PRCs.[14,29–31] The molar abundance of Crumbs (Crb) was 1.54 ± 0.34 fmole/eye (Table S3, Supporting Information), which was 173-fold lower than the abundance of Opsin.

2.4. Molar Ratios of Proteins Involved in Phototransduction Cascade and PRC Organization

The 8 photoreceptor cells (schematized in **Figure 4**) in the fly eye are specialized for phototransduction (PT). We asked what molar composition of proteins involved in the PT and PRC is required for the proper functionality of the eye? The median %CV for all calculated ratios adjusted using a statistical model of error propagation[32] was close to 25% (Figure S3A, Supporting Information) and followed the same trend as biological variations.

In the PT cascade light activates Rhodopsin 1 (Rh1) that, in turn, binds and activates Gαq. This, in turn, activates NorpA (encoding phospholipase C, PLC) that generates signaling intermediates DAG (diacyl glycerols) and InsP3 (inositol 1,4,5-triphosphate) and opens the calcium-permeable TRP (Transient Receptor Potential) channels. The resulting calcium influx converts light into an electrical response.[12,33] The signal is quenched by arrestins (Arr1 and Arr2) with the help of the myosin NinaC.[34,35]

By quantifying molar abundances of these proteins in WT flies, we determined the molar ratio of 100:12:4 for Opsin-1: NorpA: TRP (Figure 4). It was previously suggested that the abundance of TRP and NorpA is within the range of 8% to 15% of Opsin-1,[36] which is consistent with their role as amplifiers and transducers of signals triggered by Opsin-1. It is also close to the molar ratios previously determined in the amphibian retina: 100: 10: 0.6 for Rhodopsin: G-protein: Phosphodiesterase (PDE).[37] Arr2 protein was ≈3.5 times more abundant than Arr1 (Figure 4), which also corroborated with the previous reports.[38,39] The molar ratio of NinaC, which helps in translocating signal quenching proteins Arrestins, to Opsin-Rh1 was 100: 36 (Opsin-Rh1:NinaC) (Figure 4). Taken together, Opsin (the protein component of Rh1), which is responsible for initiation of the PT cascade, was present in higher molar ratio when compared to other proteins, thus corroborating previous estimates obtained by means of classical biochemistry.

A genetic network comprising *crb, chp, prom,* and *eys* plays an important role in shaping and maintaining the rhabdomere,[40] which prompted us to determine their molar ratios (Figure 4). The Crumbs complex consists of an evolutionarily conserved group of proteins, including the central constituent Crb, associated with the scaffolding proteins Stardust, Patj, and *D*Lin-7.[31] Peptides from Patj and Stardust were not included into the chimera standard because they were not detected by pilot experiments (data not shown). The molar ratio of Crb and *D*Lin-7 was 1:3 (Figure 4).

MS Western quantification also encompassed a network that controls rhabdomere shaping. The molar ratio of Crb: Eys: Prom: Chp per cell was 1:25:3:116 (Figure 4). Interestingly, Crb was the least abundant among these proteins, which reflects the small size of the sub-apical domain (stalk membrane) to which Crumbs localizes. Eys is secreted into the interrhabdomeral space, is shared between all rhabdomeres and is 25 times more abundant than Crb. Proteins such as Chp and Prom, which associate with the largest domain of the apical membrane, the rhabdomere, are even more abundant, with Chp being considerably more abundant than Prom. These molar ratios are consistent with the restricted localization of Prom to only the tips of the microvilli in the rhabdomere, while Chp is spread within the entire rhabdomere.[41] Hence, Crb is a sub-stoichiometric component compared to other proteins in this network.

2.5. Linking Phenotype to Genotype through Molecular Abundance of Eye Proteins

We next applied MS Western to quantify proteins of eyes from flies with mutated *crumbs* (*crb*). These mutants are well

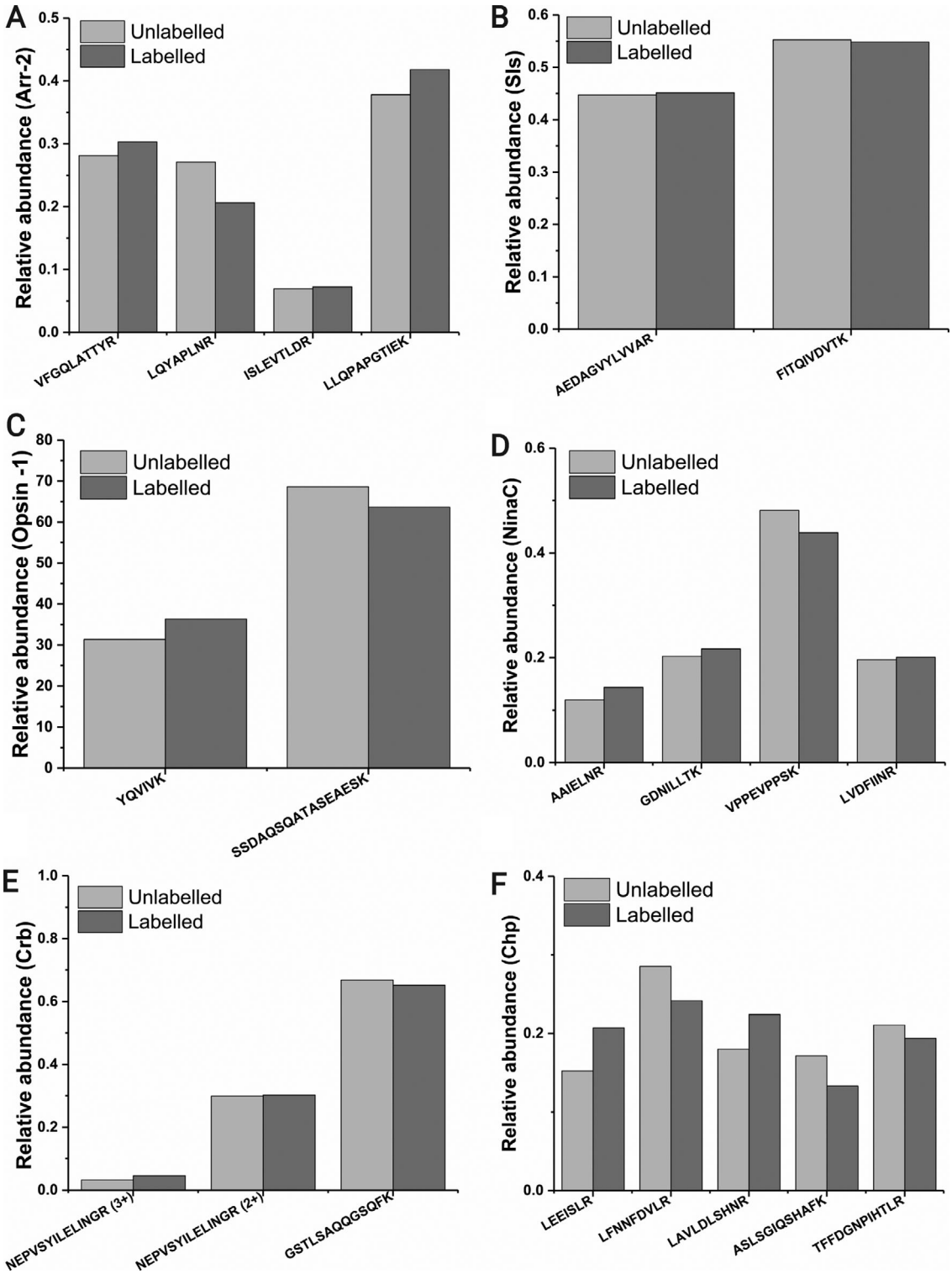

Figure 3. Relative abundances of endogenous and chimeric peptides. A–D) Relative abundances of labelled (standards) and unlabeled (endogenous) peptides of Arrestin-1 (Arr-2), Titin (Sls), Opsin-1 (NinaE), neither inactivation nor afterpotential (NinaC), Crumbs (Crb), and Chaoptin (Chp). Peptide abundances are normalized to the sum of abundances of all proteotypic peptides from the endogenous or from the chimera proteins, respectively. They are independent from the amount of protein.

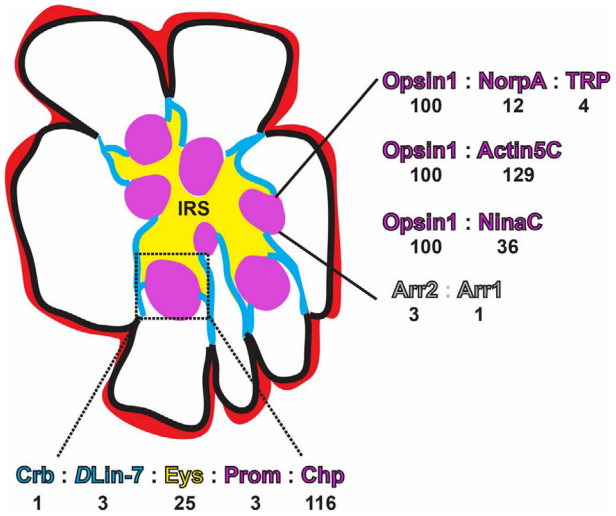

Figure 4. Summary of stoichiometric ratios of functionally relevant eye proteins. Schematic of an ommatidium representing seven photoreceptor cells (PRCs) with their apical/Rhabdomere (magenta), sub-apical (blue), basal (black) membrane domains, interrhabdomeral space (IRS; yellow), and the surrounding pigment cells (red). Stoichiometries are indicated below the proteins of interest with roles in phototransduction and/or in organizing the PRC. Protein names are color-coded to indicate their subcellular association. Stoichiometries were calculated using the fmole/cell amounts of proteins except for Arr1, Arr2, and Actin5C where fmole/eye were used.

characterized in terms of their genetic lesion and phenotype. Two of these, crb^{11A22} (null allele) and crb^{8F105} (point mutation encoding a truncated protein lacking 23 amino acids), display abnormal PRC morphology in adult eyes, with bulky and closely apposed rhabdomeres[14–16] (**Figure 5**A–D). Of these two alleles, crb^{11A22} displays a more severe phenotype both in terms of bulkiness of the distal part of rhabdomeres and defects in their proximal extension. In contrast, crb^{p13A9}, which contains a mutation that eliminates only one of three isoforms, the Crb_C isoform, induces no apparent morphological abnormalities[42] (Figure 5D). This has raised two long standing questions: i) how does overall levels of Crumbs in these mutant alleles correlate with the severity of rhabdomere phenotype, and ii) does abnormal shape of the rhabdomeres in *crb* mutants correlate with altered levels of rhabdomeric proteins such as Opsin, Trp, or Chp?

Molar abundance of Crb corroborated our expectations for the different genetic lesions: crb^{11A22} is a protein null allele and, accordingly, the protein was not detected (Figure 5E). The crb^{8F105} mutation induces a premature stop codon, resulting in a truncated protein lacking the C-terminal 23 amino acids.[43] In line with this, we detected, on average, 0.4 ± 0.1 fmoles Crb protein/eye in crb^{8F105} as compared to 1.0 ± 0.1 fmoles/eye in control flies. This is significantly less than in controls, but more than in the null mutant and reflects the difference in severity of the mutant phenotype. Antibodies against Crb that are typically used in Western blotting and immunostaining experiments are targeted to the extracellular domain, which is intact in the crb^{8F105} allele. But they did not allow exact quantification. Therefore, the molar levels obtained for these alleles (Figure 5E) help to associate Crb abundances to the severity of their phenotypes. This result can now be applied to other mutants with defects in members of the Crb complex, which affect the morphology of the rhabdomeres.

The third mutant (crb^{p13A9}) lacks the Crb_C isoform whilst producing Crb_A and Crb_B/D in pupal and adult eyes.[42] The quantitypic peptides used for the quantification of Crb were from the extracellular domain and is shared by all four isoforms. Yet, the total protein level did not change (Figure 5E), suggesting that one of the other isoforms may be upregulated. Interestingly, *D*Lin-7, one of the core components of the Crb complex, had the same abundance in the two more severely affected alleles (Figure 5E). This might reflect the mosaic nature of these mutants and/or the contribution of the postsynaptic *D*Lin-7[44] to these values in the eye.

2.6. Changes in Molecular Organization Following Abnormal PRC Development in *crumbs* Mutants

Since most *crb* mutants have abnormally shaped rhabdomeres that do not extend completely,[14–16] we next asked whether the levels of rhabdomeric proteins are changed in these mutants. First, we considered the members of the PT network, many of which are present in the rhabdomere. Intriguingly, we found that despite the gross abnormalities in rhabdomeres in crb^{11A22} and crb^{8F105}, overall levels of most of the phototransduction proteins, that is, Opsin 1, Trp, NorpA, Arr1, and Arr2, were unchanged, whereas Gαq was increased in crb^{8F105} only (Figure 5F). Thus, rhabdomere shape changes in *crb* mutant alleles did not correlate with the abundance of PT proteins. Proteins that are known to shape the rhabdomere, for example, Prom and Chp also did not change across the alleles (Figure 5G). We learned from previous studies that Chp[40] and Rh1[45] are mislocalized in *crb* mutants. However, using our technique we can confidently say that the molar abundance of Chp does not change (Figure 5G), showing that the overall levels of these proteins are not altered when rhabdomeres are abnormally shaped. In contrast, Eys is significantly reduced in crb^{11A22} eyes (Figure 5G). This provides a molecular explanation for the observation of fusion of adjacent rhabdomeres in crb^{11A22}(Figure 5B), a phenotype reminiscent to rhabdomeres in *eys* mutants, which are completely fused.[41,46]

Immunostaining data (Figure S3C–F, Supporting Information) corroborate our findings that Eys, which is secreted into the inter rhabdomeral space (IRS, Figure S3B, Supporting Information), is reduced in crb^{11A22} but not in other *crb* alleles. Because crb^{11A22} is the only mutant allele here that completely lacks the extracellular domain, reduced Eys levels might reflect the importance of the extracellular domain of Crb in Eys secretion and/or stabilization and in the formation of the IRS. Indeed genetic evidence indicated that overexpression of the extracellular domain alone can rescue some of the rhabdomeric defects in these *crb* mutants.[47] NinaC is significantly increased in the two alleles with abnormally shaped rhabdomeres (Figure 5F). NinaC is a photoreceptor-specific unconventional Myosin, which binds to Actin filaments[48] and is required for the Ca^{+2}-dependent termination of phototransduction[49,50] and the translocation of signaling proteins like Gαq and Arr2 to the rhabdomeres.[49,51,52] Interestingly, mutants in *ninaC* also exhibit abnormalities in cytoskeletal organization of the rhabdomeres[35] and display smaller rhabdomeres[35,53] during development. Thus,

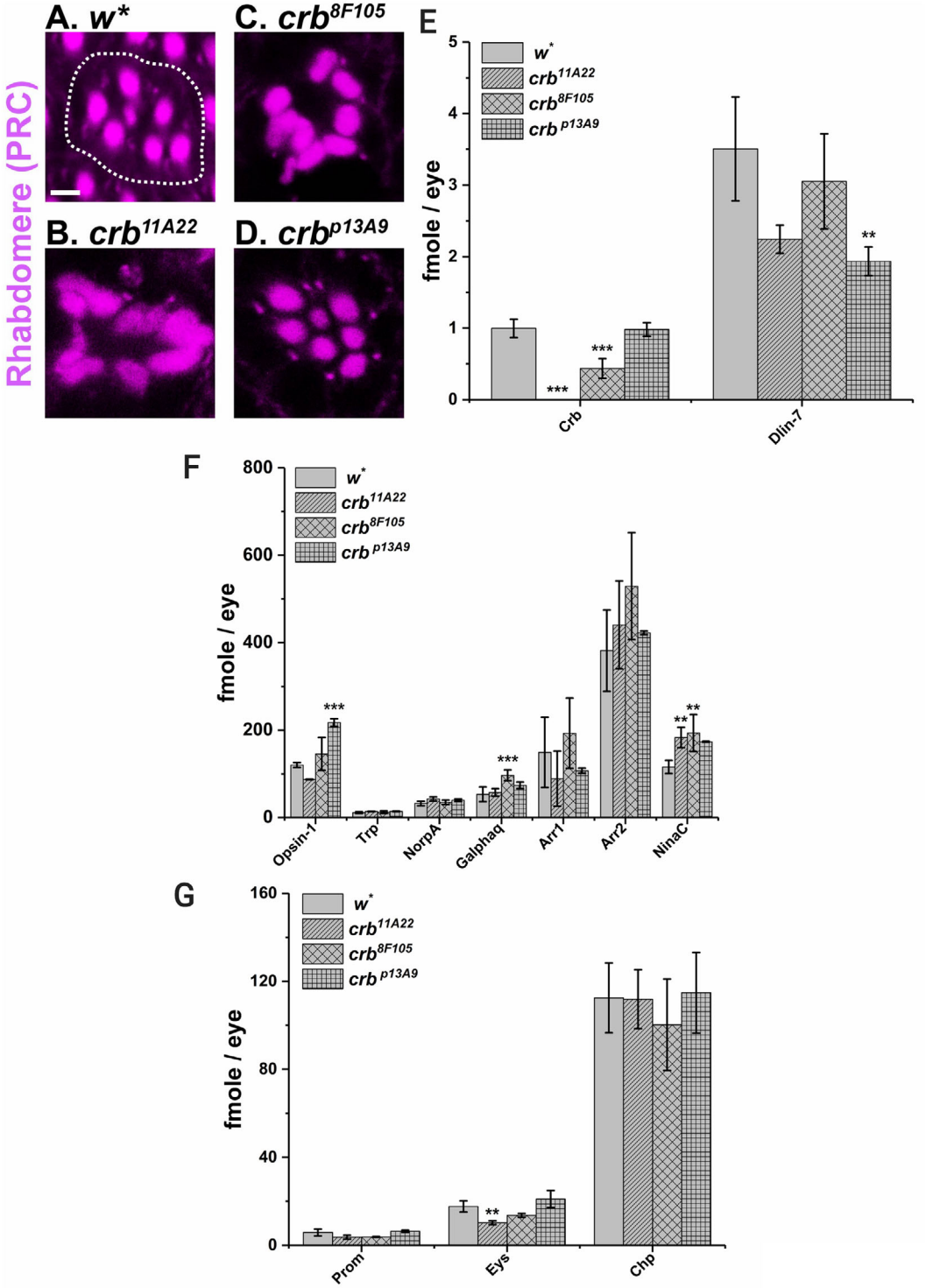

Figure 5. Absolute quantification of eye proteins in *crb* mutants. A–D) 1 µm optical slices of confocal images of cross sections of adult flies, labelled with fluorescently tagged Phalloidin, which labels the apical domain of PRCs (rhabdomere). In the control (A, w^*), the rhabdomeres of 7 PRCs are distinctly separated and clearly evident. In contrast, in crb^{8F105} (C) and crb^{11A22} (B) mutant eyes the rhabdomeres are bulky in appearance and are in close proximity to each other. A mutant in the *crb_C* isoform crb^{p13A9} does not exhibit morphological defects in the rhabdomeres (D). Scale = 2 µm. E–G) Fmole/eye of E) Crumbs and *D*Lin-7, F) photo-transduction proteins (7 proteins) G) Prom, Eys, and Chp in the different *crb* alleles. The data is represented as means ± standard deviation (S.D.) of 2 biological replicates with two technical replicates each. *p*-values represent $p > 0.05$ (ns), $p \leq 0.05$ (*), $p \leq 0.01$ (**), $p \leq 0.001$ (***), $p \leq 0.0001$ (****). One way ANNOVA was performed with Holm–Bonferroni statistical method.

significantly increased levels of NinaC in crb^{11A22} and crb^{8F105} as compared to controls might be relevant in the context of the role of Crb in rhabdomere shape.

2.7. Quantitative Changes of Proteins in *crb* Mutant Alleles

We have sorted the quantified proteins into six classes (Table S6, Supporting Information) based on changes in their molar abundance as compared to controls. Class I includes six proteins whose levels were significantly changed across all three *crb* mutant alleles. Three out of these six proteins have predicted functions attributed to ER stress (CG11594) or they participate in oxidation-reduction reactions across membranes (Etf-QO, CG3699). This is especially interesting because Crumbs controls NADPH Oxidase and thereby impacts the levels of reactive oxygen species[54] in tissues. In fact, *crb* mutant adult's eyes exhibit high oxidative stress. In the future it will be interesting to evaluate if these three proteins are part of the redox homeostasis mechanisms in *crb* alleles.

Class II includes four proteins that are significantly changed in only those alleles that have an obvious developmental defect (namely crb^{11A22} and crb^{8F105}). Two out of these four proteins (GstE3 and GstD3) are linked to the oxidative stress response. A third protein (CG11208) is implicated in fatty acid oxidation and might constitute an interesting candidate to examine the metabolic consequences of altered Crumbs function.

Class III includes proteins that are significantly changed in only those *crb* alleles that affect the extracellular domain, which is either completely absent (crb^{11A22}) or modified (crb^{p13A9}, which lacks the Crb_C isoform with a different extracellular domain). Both these alleles exhibit severe light-induced degeneration, unlike crb^{8F105}.[14] Note that our analyses were performed on flies that were reared under conditions which do not cause retinal degeneration. Therefore, any changes observed in both these alleles constitute pre-degenerative changes and can be hypothesized to be causally linked to degeneration induced by the loss of *crumbs*. Significant changes are observed in a microtubule associated protein (Map205), an actin linker protein (Bent, isoform F), and in an endomembrane protein (Ugt86Da), in both crb^{11A22} and crb^{p13A9}. These data open the interesting possibility to test the hypothesis of a link between the extracellular domain of Crumbs and retinal degeneration.

Class IV includes proteins that are significantly changed in only one out of the three alleles and reflect allele-specific changes. The most interesting amongst these is Eys described in the previous section, which is only affected in crb^{11A22}. Likewise, changes in Gαq and Moesin in crb^{8F105} might reflect the consequence of the specific lack of the C-terminal amino acids of the intracellular domain and will be candidates for future investigation in this regard. In fact, Crb has been shown to bind to Moesin via its FERM-binding domain, which is affected in crb^{8F105}.[55] crb^{p13A9} shows very interesting allele-specific changes including Actin, Twinstar (Tsr), an actin depolymerizing factor, and Veli/*D*-Lin7. Particularly surprising are the changes in Veli/*D*-Lin7, a core member of the Crb protein complex.[56] This apparent discrepancy is most likely due to the mosaic nature of the tissue in crb^{11A22} and crb^{8F105}, which still include small patches of wild-type cells that may contribute to nullifying any effects observed in these mutants. Nevertheless, all proteins changed in the allele lacking the *crb_C* isoform constitute interesting candidates in the connection of the Crumbs function in organizing the cytoskeleton.

Class V includes proteins with changes in two seemingly distinct alleles (crb^{8F105} and crb^{p13A9}). They could reflect changes in proteins upon moderate alterations of Crb levels. Class VI reflects proteins whose absolute levels are unchanged in the *crb* mutants tested here. This does not rule out a connection between Crumbs function and these proteins since our method does not offer spatial information in terms of localization of these proteins.

3. Conclusions and Perspectives

Absolute quantification of proteins in the two networks important for eye morphogenesis revealed how molar ratios are related to the molecular organization of the eye. Our study, which included wild-type flies and few mutant alleles, provided consistent values for several proteins at one-go using the MS Western workflow. Effectively, it argues against a common perception that molar abundances of proteins not associated in stable complexes are variable and inconclusive. By showing good concordance with classical biochemistry our work advocates for changing the field paradigm from mostly relative to mostly absolute quantification. Though MS Western lacks spatial resolution, it can be used in conjunction with various imaging techniques combining the power of absolute quantification and accurate localization of target proteins.

Absolute (molar) levels of proteins in cells and tissues is a resource of quantitative descriptors. With predictive biology becoming one of the key facets of biology, this study provides an important resource to make it possible. It also adds a novel possibility to quantitatively compare phenotypes of different alleles and thus contribute unravelling the function of genes.

4. Experimental Section

Animals: All *Drosophila melanogaster* lines and crosses were maintained on a cornmeal-yeast based culture medium at 25 °C in a 12 h light-dark cycle, with light intensity ranging from 600–1000 lux. This light exposure paradigm causes no light-induced retinal degeneration in the genotypes under consideration.[14,42] *Oregon R* was the wild-type strain of choice. The genetic control were white-eyed flies of the genotype *white** (*w**). The following *crb* alleles were used: crb^{11A22}[57] crb^{8F105},[57] crb^{p13A}[42]. Genetic eye mosaics consisting of large mutant patches of crb^{11A22} and crb^{8F105} were generated by crossing *yw*eyFLP;;FRT82B w+ cl3R3/TM6B males*[58] to *w*; FRT82B* crb^{11A22}*/TM6B* and *w*; FRT82B* crb^{8F105}*/TM6B* respectively.

Immunostaining: *Drosophila* eyes were processed for electron microscopy and cryosectioning, immunostaining, and confocal imaging as described in ref. [42]. Rhabdomeres were visualized with fluorescently conjugated phalloidin (Thermo Fisher Scientific). The primary antibody used was mouse Anti-Eys/Spam (21A6, deposited by Benzer, S[41]) and was obtained from the Developmental Studies Hybridoma Bank, created by the NICHD of the NIH and maintained at The University of Iowa, Department of Biology, Iowa City, IA 52 242.

Absolute Quantification by MS Western: Absolute quantification of proteins was performed by the method of MS Western[9] (Figure S1, Supporting Information). Eyes of 3–5 days old *Drosophila* females of each genotype were dissected to a total of 40 per biological replicate and lysed according to Kumar et al.,[9] in a buffer consisting of 50 mM Tris-HCl (pH 7.5), 1 mM EDTA, 0.7% (v/v) Triton X-100, 0.2% (w/v)

3-[(3-Cholamidopropyl)dimethylammonio)-1-propanesulfonate (CHAPS), 0.1% Octylglucoside (OGP), 150 mM NaCl with protease inhibitor cocktail (Roche, Germany) and then snap frozen in liquid nitrogen for later analysis. The frozen eyes were thawed on ice and crushed using a micro hand mixer (Carl Roth, Germany). The crude extract was then centrifuged for 15 min at 13 000 rpm and 4 °C to remove tissue debris. The clear supernatant was then transferred to a fresh Protein Lo-Bind tube (Eppendorf, Hamburg, Germany). The total protein content from the eyes was loaded on a precast 4–20% gradient 1-mm thick polyacrylamide mini-gels from Anamed Elektrophorese (Rodau, Germany) for 1D SDS PAGE. Separate gels were run for 1 pmol of BSA and isotopically labeled chimeric standard containing 3–5 unique quantitypic peptides per each of 43 eye proteins.[9] Quantitypic peptides were selected in preliminary semi-quantitative LC-MS/MS analyses of eye extracts; they contained no methionine and cysteine amino acid residues and mis-cleaved tryptic sites. The unique peptides were assembled into a synthetic gene construct and were expressed in ΔLys ΔArg auxotrophic strain of *E.coli* supplemented with $^{15}N_7$, $^{13}C_6$-Arginine, and $^{13}C_6$ –Lysine[9] to yield a 264 kDa chimeric protein (CP). Proteins were quantified in two biological replicas, each of which was analyzed in two technical replicates. Since molecular weights of the target proteins were within 15–200 kDa range, extracts of eye proteins were pre-separated by 1D SDS PAGE, stained with Coomassie and gel slabs cut in six slices. Each slice was co-digested with the bands of 264 kDa CP and reference protein BSA using trypsin (Trypsin Gold, mass spectrometry grade from Promega, Madison) and recovered peptides were analyzed by LC-MS/MS. MS/MS spectra were acquired in the data-dependent acquisition mode on a Q Exactive HF (Thermo Fisher Scientific, Bremen, Germany) mass spectrometer interfaced with a Dionex Ultimate 3000- HPLC system (Thermo Scientific, Bremen, Germany) equipped with a 300 μm i.d × 5mm trap column and a 75 μm × 15 cm PepMap 100 C18 column under the conditions and instruments settings provided in Table S2, Supporting Information.

Database Searches and Data Processing: Peptide were matched by Mascot v.2.2.04 software (Matrix Science, London, UK) by searches against *Drosophila melanogaster* (December 2019; 21 973 proteins) Uniprot protein sequence database. Precursor mass tolerance was 5 ppm and fragment mass tolerance was 0.03 Da; fixed modification: carbamidomethyl (C); variable modifications: acetyl (protein N terminus), oxidation (M); labels: $^{13}C(6)$ (K) and $^{13}C(6)^{15}N(4)$ (R); cleavage specificity: trypsin, with up to two missed cleavages allowed. Peptides having the ions score above 15 were accepted ($p < 0.05$). The chromatographic alignment and feature detection were carried using Progenesis LC-MS v.4.1 (Nonlinear Dynamics, UK). The absolute quantification was performed by calculating the abundances of corresponding labelled and unlabeled peptides using an in-house software MS Western Mass Filter. The statistical analysis was carried out in OriginLab 2017 (OriginLab Corp, Northampton MA).

Software-Assisted Absolute Quantification of Proteins by MS Western: MS Western Mass Filter is a stand-alone Java-script based application that uses in-memory SQL database (ref: https://github.com/agershun/alasql) for fast access and search in the CSV file. The database entries are presented through data table component (ref: https://datatables.net/). MS Western Mass Filter runs on a workstation with 16 GB RAM and 4-cores processor under Windows 7. All identified peptides are exported from Progenesis LC-MS v.4.1 (Nonlinear Dynamics, UK) as a .csv file reporting matched peptide sequences, *m/z*, retention time and raw integrated peak abundances. The list of quantitypic peptides and reference (BSA) peptides with known molar amounts are organized in a separate tab. The software matches standard, endogenous and reference peptides, calculates the molar amounts of proteins and reports them in a tabular format. It is available for free download at: https://github.com/bharathkumar91/MSWestern-MZ

Image Processing and Figure Panel Generation: Microscopy images were processed using ImageJ/Fiji[59] for making projections of the z-stacks and Adobe Photoshop CS5.1 for adjusting brightness and contrast. Adobe Illustrator CS3 was used for image assembly. The figures were then assembled using Biorender.com. The MS western workflow figure was also created using Biorender.com.

Data Availability: Raw data have been deposited to the ProteomeXchange Consortium via the PRIDE partner repository with the dataset identifier PXD018001.

Supporting Information

Supporting Information is available from the Wiley Online Library or from the author.

Acknowledgements

Work in E.K. and A.S. groups was supported by the Max Planck Society. B.K.R. is a member of the International Max Planck Research School for Cell, Developmental, and Systems Biology and a doctoral student at Technische Universität Dresden. The authors thank the light microscopy and electron microscopy facilities of the MPI-CBG for guidance. The authors are grateful for the members of A.S. and E.K. groups for expert technical support and useful discussions.

Open access funding enabled and organized by Projekt DEAL.

Conflict of Interest

The authors declare no conflict of interest.

Author Contributions

B.K.R. and S.H. contributed equally to this work. S.H. and E.K. designed the experiments involving *Drosophila* and SH performed these experiments. M.K. designed and expressed the chimeric construct used for quantification. B.K.R. and A.S. designed the MS Western analysis and B.K.R. performed the experiment. B.K.R., S.H., E.K., and A.S. analyzed and interpreted the data. H.K.M. and I.H. conceptualized and developed the quantification software. B.K.R., S.H., E.K., and A.S. wrote the manuscript.

Keywords

absolute quantification of proteins, *Drosophila* eye, morphogenesis, MS Western, rhabdomere

Received: January 24, 2020
Revised: May 29, 2020
Published online: September 3, 2020

[1] E. Ahrné, L. Molzahn, T. Glatter, A. Schmidt, *Proteomics* **2013**, *13*, 2567.
[2] R. E. Higgs, M. D. Knierman, V. Gelfanova, J. P. Butler, J. E. Hale, **2005**, 1442.
[3] K. A. Neilson, N. A. Ali, S. Muralidharan, M. Mirzaei, M. Mariani, G. Assadourian, A. Lee, S. C. van Sluyter, P. A. Haynes, *Proteomics* **2011**, *11*, 535.
[4] M. Brönstrup, *Expert Rev. Proteomics* **2004**, *1*, 503.
[5] K. Kito, T. Ito, *Curr. Genomics* **2008**, *9*, 263.
[6] B. J. Smith, D. Martins-de-Souza, M. Fioramonte, *Methods Mol. Biol.* **2019**, 3.
[7] J. A. Ankney, A. Muneer, X. Chen, *Annu. Rev. Anal. Chem.* **2018**, *11*, 49.

[8] H. Taymaz-Nikerel, A. R. Lara, *Front. Bioeng. Biotechnol.* **2016**, *4*.
[9] M. Kumar, S. R. Joseph, M. Augsburg, A. Bogdanova, D. Drechsel, N. L. Vastenhouw, F. Buchholz, M. Gentzel, A. Shevchenko, *Mol. Cell. Proteomics* **2018**, *17*, 384.
[10] M. Lehmann, E. Knust, S. Hebbar, in *Methods Mol. Biol.*, Humana Press Inc. **2019**, 221.
[11] C. Montell, *Trends Neurosci.* **2012**, *35*, 356.
[12] C. Montell, *Annu. Rev. Cell Dev. Biol.* **1999**, *15*, 231.
[13] R. C. Hardie, *J Exp Biol* **2001**, *204*, 3403.
[14] K. Johnson, F. Grawe, N. Grzeschik, E. Knust, *Curr. Biol.* **2002**, *12*, 1675.
[15] M. Pellikka, G. Tanentzapf, M. Pinto, C. Smith, C. J. McGlade, D. F. Ready, U. Tepass, *Nature* **2002**, *416*, 143.
[16] S. Izaddoost, S. C. Nam, M. A. Bhat, H. J. Bellen, K. W. Choi, *Nature* **2002**, *416*, 178.
[17] C. Lawless, S. W. Holman, P. Brownridge, K. Lanthaler, V. M. Harman, R. Watkins, D. E. Hammond, R. L. Miller, P. F. G. Sims, C. M. Grant, C. E. Eyers, R. J. Beynon, S. J. Hubbard, *Mol. Cell. Proteomics* **2016**, *15*, 1309.
[18] K. M. Carroll, D. M. Simpson, C. E. Eyers, C. G. Knight, P. Brownridge, W. B. Dunn, C. L. Winder, K. Lanthaler, P. Pir, N. Malys, D. B. Kell, S. G. Oliver, S. J. Gaskell, R. J. Beynon, *Mol. Cell. Proteomics* **2011**, *10*, M111.007633.
[19] J. E. O'Tousa, W. Baehr, R. L. Martin, J. Hirsh, W. L. Pak, M. L. Applebury, *Cell* **1985**, *40*, 839.
[20] J. P. Kumar, D. F. Ready, *Development* **1995**, *121*, 4359.
[21] R. J. Sapp, J. S. Christianson, L. Maier, K. Studer, W. S. Stark, *Exp. Eye Res.* **1991**, *53*, 73.
[22] J. Nie, S. Mahato, A. C. Zelhof, *PLoS Genet.* **2014**, *10*, e1004608.
[23] D. F. Ready, T. E. Hanson, S. Benzer, *Dev. Biol.* **1976**, *53*, 217.
[24] N. J. Scavarda, J. O'Tousa, W. L. Pak, *Proc. Natl. Acad. Sci. USA* **1983**, *80*, 4441.
[25] R. C. Hardie, Springer, Berlin, Heidelberg **1985**, 1.
[26] T. Wang, C. Montell, *Pflugers Arch. Eur. J. Physiol.* **2007**, *454*, 821.
[27] N. Muschalik, E. Knust, *J. Cell Sci.* **2011**, *124*, 3715.
[28] M. Pellikka, U. Tepass, *J. Cell Sci.* **2017**, *130*, 2147.
[29] M. Mishra, M. Rentsch, E. Knust, *Eur. J. Cell Biol.* **2012**, *91*, 706.
[30] M. Leslie, *J. Cell Biol.* **2012**, *198*, 954.
[31] N. A. Bulgakova, E. Knust, *J. Cell Sci.* **2009**, *122*, 2587.
[32] D. T. Holmes, K. A. Buhr, *Clin. Biochem.* **2007**, *40*, 728.
[33] R. C. Hardie, P. Raghu, *Nature* **2001**, *413*, 186.
[34] J. L. Hicks, D. S. Williams, *J. Cell Sci.* **1992**, *101*, 247.
[35] H. Matsumoto, K. Isono, Q. Pye, W. L. Pak, *Proc. Natl. Acad. Sci. USA* **1987**, *84*, 985.
[36] A. Huber, P. Sander, R. Paulsen, *J. Biol. Chem.* **1996**, *271*, 11710.
[37] E. N. Pugh, T. D. Lamb, *BBA - Bioenerg.* **1993**, *1141*, 111.
[38] B. - H. Shieh, I. Kristaponyte, Y. Hong, *J. Biol. Chem.* **2014**, *289*, 18526.
[39] I. Kristaponyte, Y. Hong, H. Lu, B. - H. Shieh, *J. Neurosci.* **2012**, *32*, 10758.
[40] N. Gurudev, M. Yuan, E. Knust, *Biol. Open* **2014**, *3*, 332.
[41] A. C. Zelhof, R. W. Hardy, A. Becker, C. S. Zuker, *Nature* **2006**, *443*, 696.
[42] S. Spannl, A. Kumichel, S. Hebbar, K. Kapp, M. Gonzalez-Gaitan, S. Winkler, R. Blawid, G. Jessberger, E. Knust, *Biol. Open* **2017**, *6*, 165.
[43] A. Wodarz, F. Grawe, E. Knust, *Mech. Dev.* **1993**, *44*, 175.
[44] S. F. Soukup, S. M. Pocha, M. Yuan, E. Knust, *Curr. Biol.* **2013**, *23*, 1349.
[45] S. M. Pocha, A. Shevchenko, E. Knust, *J. Cell Biol.* **2011**, *195*, 827.
[46] N. Husain, M. Pellikka, H. Hong, T. Klimentova, K. M. Choe, T. R. Clandinin, U. Tepass, *Dev. Cell* **2006**, *11*, 483.
[47] M. Richard, N. Muschalik, F. Grawe, S. Özüyaman, E. Knust, *Eur. J. Cell Biol.* **2009**, *88*, 765.
[48] J. A. Porter, M. Yu, S. K. Doberstein, T. D. Pollard, C. Montell, *Science (80-.).* **1993**, *262*, 1038.
[49] H. S. Li, J. A. Porter, C. Montell, *J. Neurosci.* **1998**, *18*, 9601.
[50] J. A. Porter, B. Minke, C. Montell, *EMBO J.* **1995**, *14*, 4450.
[51] M. A. Cronin, F. Diao, S. Tsunoda, *J. Cell Sci.* **2004**, *117*, 4797.
[52] S. J. Lee, C. Montell, *Neuron* **2004**, *43*, 95.
[53] N. E. Baker, K. Moses, D. Nakahara, M. C. Ellis, R. W. Carthew, G. M. Rubin, *J. Neurogenet.* **1992**, *8*, 85.
[54] F. J. M. Chartier, E. J. L. Hardy, P. Laprise, *J. Cell Biol.* **2012**, *198*, 991.
[55] Z. Wei, Y. Li, F. Ye, M. Zhang, *J. Biol Chem.* **2015**, *290*, 11384.
[56] A. Bachmann, F. Grawe, K. Johnson, E. Knust, *Eur. J. Cell Biol.* **2008**, *87*, 123.
[57] G. Jürgens, E. Wieschaus, C. Nüsslein-Volhard, H. Kluding, *Wilhelm Roux's Arch. Dev. Biol.* **1984**, *193*, 283.
[58] T. P. Newsome, B. Åsling, B. J. Dickson, *Development* **2000**, *127*, 851.
[59] J. Schindelin, I. Arganda-Carreras, E. Frise, V. Kaynig, M. Longair, T. Pietzsch, S. Preibisch, C. Rueden, S. Saalfeld, B. Schmid, J. Y. Tinevez, D. J. White, V. Hartenstein, K. Eliceiri, P. Tomancak, A. Cardona, *Nat. Methods* **2012**, *9*, 676.
[60] P. Brownridge, S. W. Holman, S. J. Gaskell, C. M. Grant, V. M. Harman, S. J. Hubbard, K. Lanthaler, C. Lawless, R. O'cualain, P. Sims, R. Watkins, R. J. Beynon, *Proteomics* **2011**, *11*, 2957.
[61] R. J. Bennett, D. M. Simpson, S. W. Holman, S. Ryan, P. Brownridge, C. E. Eyers, J. Colyer, R. J. Beynon, *Sci. Rep.* **2017**, *7*, 45570.
[62] N. Takemori, A. Takemori, Y. Tanaka, Y. Endo, J. L. Hurst, G. Gómez-Baena, V. M. Harman, R. J. Beynon, *Mol. Cell. Proteomics* **2017**, *16*, 2169.